PLASMON MODES IN THREE-LAYER GRAPHENE WITH INHOMOGENEOUS BACKGROUND DIELECTRIC

Nguyen Van Men[1*], Dong Thi Kim Phuong[1], and Truong Minh Rang[2]
[1]*An Giang University, Vietnam National University Ho Chi Minh City, Vietnam*
[2]*Student, An Giang University, Vietnam National University Ho Chi Minh City, Vietnam*
*Corresponding author: Nguyen Van Men, Email: nvmen@agu.edu.vn

Abstract

The aim of this paper is to investigate collective excitations and the damping rate in a multilayer structure consisting of three monolayer graphene sheets with inhomogeneous background dielectric at zero temperature within random-phase approximation. Numerical results show that one optical branch and two acoustic ones exist in the system. The lowest frequency branch disappears as touching single-particle excitation area boundary while two higher frequency branches continue in this region. Calculations also illustrate that the frequency of optical (acoustic) mode(s) decreases (increase) as interlayer separation increases. The inhomogeneity of background dielectric and the imbalance in the carrier density in graphene sheets decline significantly plasmon frequencies in the system. Therefore, it is meaningful to take into account the effects of inhomogeneous background dielectric when calculating collective excitations in three-layer graphene structures.

Keywords: *Collective excitations, inhomogeneous background dielectric, random–phase–approximation, three-layer graphene systems.*

PHỔ PLASMON TRONG HỆ BA LỚP GRAPHENE VỚI ĐIỆN MÔI NỀN KHÔNG ĐỒNG NHẤT

Nguyễn Văn Mện[1*], Đồng Thị Kim Phượng[1] và Trương Minh Rạng[2]
[1]*Trường Đại học An Giang, Đại học Quốc gia Thành phố Hồ Chí Minh, Việt Nam*
[2]*Sinh viên, Trường Đại học An Giang, Đại học Quốc gia Thành phố Hồ Chí Minh, Việt Nam*
*Tác giả liên hệ: Nguyễn Văn Mện, Email: nvmen@agu.edu.vn

Tóm tắt

Bài báo này nhằm khảo sát kích thích tập thể và hấp thụ trong một cấu trúc nhiều lớp gồm ba lớp graphene với điện môi nền không đồng nhất ở nhiệt độ không tuyệt đối trong gần đúng pha ngẫu nhiên. Kết quả tính toán bằng số cho thấy một nhánh quang học và hai nhánh âm học tồn tại bên trong hệ. Nhánh có tần số thấp nhất biến mất khi chạm vào đường biên vùng kích thích đơn hạt trong khi hai nhánh có tần số cao hơn vẫn tiếp tục tồn tại trong vùng này. Các tính toán cũng cho thấy, tần số nhánh quang giảm xuống còn tần số các nhánh âm lại tăng lên khi khoảng cách các lớp tăng. Sự không đồng nhất của hằng số điện môi nền và sự mất cân bằng về mật độ hạt tải giữa các lớp graphene làm giảm đáng kể các tần số plasmon trong hệ. Do đó, việc tính đến ảnh hưởng của hằng số điện môi nền không đồng nhất khi xác định kích thích tập thể trong hệ ba lớp graphene là việc làm có ý nghĩa.

Từ khóa: *Kích thích plasmon, điện môi nền không đồng nhất, gần đúng pha ngẫu nhiên, hệ ba lớp graphene.*

1. Introduction

Graphene, a perfect two dimensional system consisting of one layer of carbon atoms arranged in honey-comb lattice, has attracted a lot of attention from material scientists in recent years because of its interesting features as well as application abilities in technology. Theoretical and experimental researches on graphene show that the different characters of quasi-particles in graphene, compared to normal two-dimensional electron gas, are chirality, linear dispersion at low energy and massless fermions. Due to these unique properties, graphene is considered a good candidate, replacing silicon materials being used in creating electronic devices (DasSarma et al., 2011; Geim and Novoselov, 2007; McCann, 2011).

Collective excitation (or collective plasmon) is one of the important properties of material because it is relevant to many technological fields, including optics, optoelectronics, membrane technology, and storage technology (Maier, 2007; Ryzhii et al., 2013; Politano et al., 2016; Politano et al., 2017). Therefore, scientists have been interested in calculations on plasmon characters of materials for many years. Collective excitations in the ordinary two-dimensional electron gas, in monolayer and in bilayer graphene at zero temperature have been studied and published intensively in the early years of the 21st century. Recent theoretical and experimental papers on graphene demonstrate that collective excitations in graphene spread from THz to visible light, so graphene is considered as a good material to create plasmonic devices operating in this range of frequency (DasSarma et al., 2011; Geim & Novoselov, 2007; Hwang & DasSarma, 2007; Sensarma, et al., 2010; Shin et al., 2015). It is well known that the Coulomb interaction between charged particles in multilayer structures lead to the significant increase in the frequency of undamped and weak-damped plasmon modes existing in the systems (Yan et al., 2012; Zhu et al., 2013; Men et al., 2019; Men, 2020). Moreover, publications on multilayer

structures also illustrate that the inhomogeneity of background dielectric has pronounced effects on plasmon modes (Badalyan & Peeters, 2012; Principi et al., 2012; Men & Khanh, 2017; Khanh & Men, 2018). However, most of previous works about multilayer graphene have neglected the contributions of this factor to plasmon characters due to different reasons (Yan et al., 2012; Zhu et al., 2013; Men et al., 2019; Men, 2020). This paper presents results calculated for collective excitations and the damping rate of respective plasma oscillations in a multilayer structure, consisting of three parallel monolayer graphene sheets, separated by different dielectric mediums in order to improve the model.

2. Theory approach

We investigate a multilayer system consisting of three parallel monolayer graphene, separated by a different dielectric medium with equal layer thickness d, as presented in Figure 1. Each graphene layer is considered as homogeneously doped graphene, so the carrier density is a constant $n_1 (i = 1 \div 3)$ over its surface. As a result, the Fermi wave vector and Fermi energy in each graphene sheet have uniform distributions.
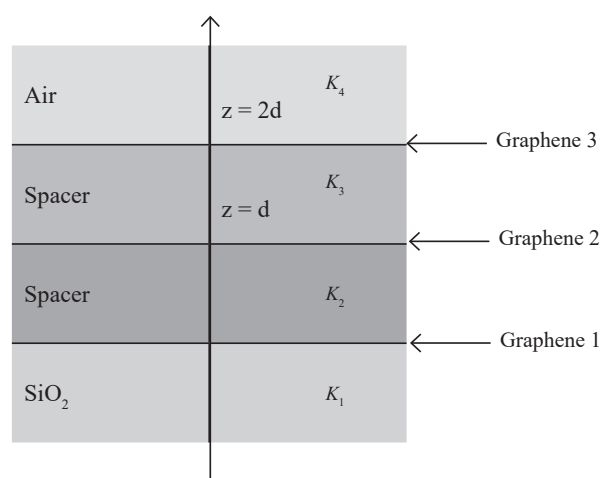
Figure 1. Three –layer graphene system with inhomogeneous background dielectric

It is well known that the plasmon dispersion relation of the system can be determined from the zeroes of dynamical dielectric function (Sarma

& Madhukar, 1981; Hwang & DasSarma, 2009; Vazifehshenas et al., 2010; Badalyan & Peeters, 2012; Zhu et al., 2013; Khanh & Men, 2018; Men & Khanh, 2017; Men et al., 2019; Men, 2020):

$$\varepsilon\left(q, \omega_p - i\gamma\right) = 0. \quad (1)$$

Where ω_p is plasmon frequency at given wave vector q, and γ is the damping rate of respective plasma oscillations. In the case of weak damping, the solutions of equation (1) can be found from the zeroes of the real part of dynamical dielectric functions as (Sarma & Madhukar, 1981; Hwang & DasSarma, 2009; Vazifehshenas et al., 2010; Badalyan & Peeters, 2012; Zhu et al., 2013; Khanh & Men, 2018; Men & Khanh, 2017; Men et al., 2019; Men, 2020):

$$\operatorname{Re} \varepsilon\left(q, \omega_p\right) = 0. \quad (2)$$

The damping rate can be calculated from the following equation:

$$\gamma = \operatorname{Im} \varepsilon\left(q, \omega_p\right)\left(\left.\frac{\partial \operatorname{Re} \varepsilon\left(q, \omega\right)}{\partial \omega}\right|_{\omega = \omega_p}\right)^{-1}. \quad (3)$$

Within random-phase approximation (RPA), the dynamical dielectric function of three-layer graphene structure is written by (Yan et al., 2012; Zhu et al., 2013; Men et al., 2019; Men, 2020):

$$\varepsilon\left(q, \omega\right) = \det\left|1 - \hat{v}\left(q\right)\hat{\Pi}\left(q, \omega\right)\right|. \quad (4)$$

Here, $\hat{v}\left(q\right)$ is the potential tensor, corresponding to Coulomb bare interactions between electrons in graphene sheets, formed from Poisson equation and read (Scharf & Matos-Abiague, 2012; Phuong & Men, 2019; Men, 2019):

$$v_{ij}\left(q\right) = \frac{2\pi e^2}{q} f_{ij}\left(q\right). \quad (5)$$

Where:

$$f_{11}\left(q\right) = \frac{2\left[\left(\kappa_2 + \kappa_3\right)\left(\kappa_3 - \kappa_4\right) + 2\kappa_3\left(\kappa_2 - \kappa_3\right)e^{2qd} + \left(\kappa_2 + \kappa_3\right)\left(\kappa_3 + \kappa_4\right)e^{4qd}\right]}{M\left(qd\right)}, \quad (6)$$

$$f_{22}\left(q\right) = \frac{8e^{2qd}\left[\kappa_1 \cosh\left(qd\right) + \kappa_2 \sinh\left(qd\right)\right]\left[\kappa_3 \cosh\left(qd\right) + \kappa_4 \sinh\left(qd\right)\right]}{M\left(qd\right)}, \quad (7)$$

$$f_{33}\left(q\right) = \frac{2\left[\left(\kappa_2 + \kappa_3\right)\left(\kappa_2 - \kappa_1\right) + 2\kappa_2\left(\kappa_3 - \kappa_2\right)e^{2qd} + \left(\kappa_1 + \kappa_2\right)\left(\kappa_2 + \kappa_3\right)e^{4qd}\right]}{M\left(qd\right)}, \quad (8)$$

$$f_{12}\left(q\right) = f_{21}\left(q\right) = \frac{8\kappa_2 e^{2qd}\left[\kappa_3 \cosh\left(qd\right) + \kappa_4 \sinh\left(qd\right)\right]}{M\left(qd\right)}, \quad (9)$$

$$f_{13}\left(q\right) = f_{31}\left(q\right) = \frac{8\kappa_2\kappa_3 e^{2qd}}{M\left(qd\right)}, \quad (10)$$

$$f_{32}(q) = f_{23}(q) = \frac{8\kappa_3 e^{2qd}\left[\kappa_2 \cosh(qd) + \kappa_1 \sinh(qd)\right]}{M(qd)} \quad , (11)$$

with

$$M(x) = (\kappa_1 - \kappa_2)(\kappa_2 + \kappa_3)(\kappa_3 - \kappa_4) + 2e^{2x}(\kappa_2 - \kappa_3)(\kappa_1\kappa_3 - \kappa_2\kappa_4) +$$
$$+ e^{4x}(\kappa_1 + \kappa_2)(\kappa_2 + \kappa_3)(\kappa_3 + \kappa_4). \tag{12}$$

$\hat{\Pi}(q,\omega)$ is the polarization tensor of the system. When electron tunneling between graphene layers can be neglected (large separation), only diagonal elements of the polarization tensor differ from zero, so

$$\hat{\Pi}(q,\omega) = \delta_{ij}\Pi_0^i(q,\omega). \tag{13}$$

In equation (13), $\Pi_0^i(q,\omega)$ is Lindhard polarization function of layer graphene at zero temperature ($i = 1 \div 3$) in the structure observed by Hwang & DasSarma (2007).

Equations (5)-(12) show the complicated dependence of Coulomb bare interactions on the inhomogeneity of background dielectric. This dependence leads to the differences in plasmon characters in an inhomogeneous three-layer graphene system, compared to homogeneous ones. The numerical results calculated for this system are demonstrated in the following.

3. Results and discussions

This section presents numerical results calculated for collective excitations in a three-layer graphene system with inhomogeneous background dielectric at zero temperature. In an inhomogeneous system, dielectric constants used are $\kappa_1 = \kappa_{SiO_2} = 3.8$, $\kappa_2 = \kappa_{Al_2O_3} = 6.1$, $\kappa_3 = \kappa_{BN} = 5.0$; $\kappa_4 = \kappa_{air} = 1.0$. In all figures, E_F and k_F are used to denote Femi energy and Fermi wave vector of the first graphene sheet.
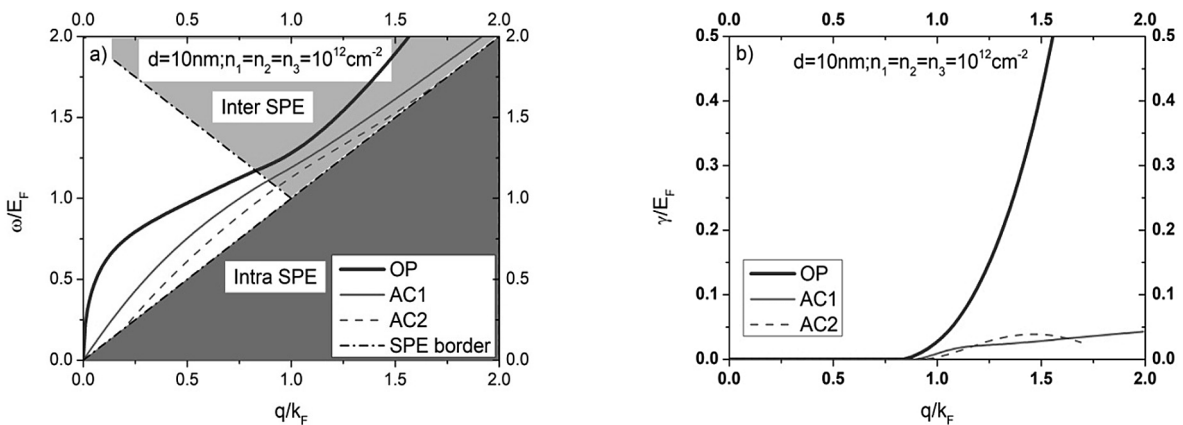
Figure 2. Plasmon modes (a) and damping rate (b) in three-layer graphene structure, plotted for $d = 10$ nm and $n_1 = n_2 = n_3 = 10^{12}$ cm^{-2}. The grey-shaded area in Figure 2(a) shows single-particle excitation area of the system

Figure 2 plots collective excitations (a) and damping rate (b) in a three-layer graphene system shown in Figure 1. Similar to other multilayer systems (Yan et al., 2012; Zhu et al., 2013; Men et al., 2019; Men, 2020), three plasmon modes exist in a three-layer graphene structure. The largest frequency branch is called optical mode (Op), corresponding to in-phase oscillations, and two smaller frequency ones are named as acoustic modes (Ac) illustrating out-of-phase oscillations of carriers in the system. The figure shows that Op and Ac1 branches continue in single-particle excitation (SPE) area while the Ac2 branch disappears as touching SPE boundaries at about $q = 1,6k_F$. The damping rate, presented in Figure 2(b), demonstrates that although Op mode (thick solid line) can continue in the SPE region, this mode loses its energy quickly as the plasmon curve goes far away from SPE boundaries. As also seen from Figure 2(b), the damping rate of the Ac2 branch increases from zero as this plasmon line crosses intra SPE region boundary, and then decreases as this line approaches inter SPE area boundary. This behavior differs sharply from that of Op and Ac2 branches. It is necessary to note that the energy loss in the Op branch is similar to that in monolayer graphene, obtained by Hwang & DasSarma (2007).
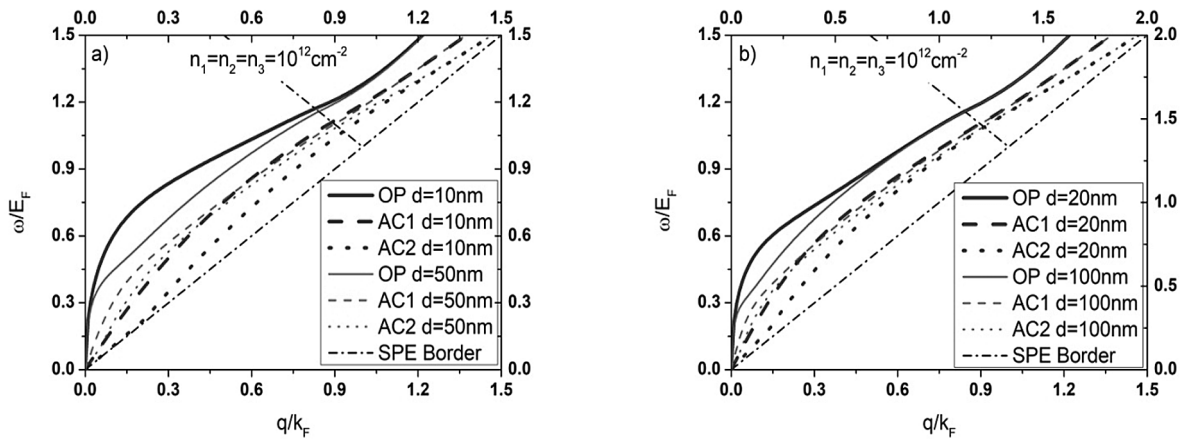
Figure 3. Collective excitations in three-layer graphene structure for several interlayer separations. Parameters used are $n_1 = n_2 = n_3 = 10^{12}$ cm^{-2}, $d = 10$ nm; 20 nm; 50 nm and $d = 100$ nm. Dashed-dotted lines present SPE boundaries

Collective excitations in a three-layer graphene system with several separations are illustrated in Figure 3. The figure shows that Op frequency decreases significantly while Ac ones increase noticeably as separation increases. The changes in frequency occur mainly nearby the Dirac points, in a small wave vector region, and outside SPE area. Nevertheless, in the case of Ac branches, plasmon frequencies increase slightly in a large wave vector region. It is seen from the figures that the increase in the interlayer distance makes Op (Ac) branch shifts down (up), especially outside SPE region. As a result, plasmon branches become closer to each other, similar to those in multilayer graphene systems with homogeneous background dielectric in which plasmon curves approach that of single-layer graphene in limit of $d \to \infty$. However, the difference between the two cases is that plasmon curves in the inhomogeneous case are still separated from each other for large separations while they are identical in the homogeneous case as observed in previous papers (Yan et al., 2012; Zhu et al., 2013; Men et al., 2019; Men, 2020).
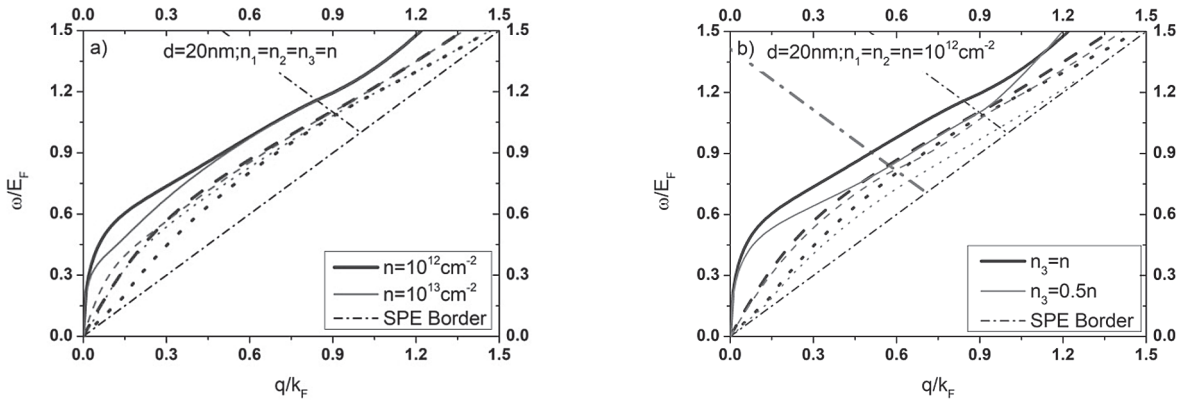
Figure 4. Plasmon modes in three-layer graphene structure for several carrier densities, ploted for $d = 20\ nm$ **Dashed-dotted lines show SPE area boundaries**

According to recent publications, carrier density has pronounced contributions to plasmon properties of layered structures (Hwang & DasSarma, 2007; Hwang & DasSarma, 2009; Badalyan & Peeters, 2012; Men & Khanh, 2017; Khanh & Men, 2018; Men et al., 2019). Figure 4 plots plasmon modes in a three-layer graphene system with the variation of carrier density in graphene sheets. Figure 4(a) demonstrates that the increase in carrier density in graphene layers declines remarkably frequency of plasmon branches, found mainly outside SPE region. Besides, the imbalance in carrier density between graphene layers causes significant effects to plasmon modes as seen from Figure 4(b). In the case of $n_3 = 0.5n_1$, the frequency of all branches

decreases noticeably, in comparison with that of $n_3 = n_1$, but at different levels. The Op branch is affected more strongly than Ac ones are. The lowest plasmon branch approaches SPE area boundary and disappears at a smaller wave vector, about $q = 1.2k_F$ compared to $1.6k_F$ in the case of equal carrier density. Moreover, as carrier density in the third layer decreases, the SPE region boundary shifts down (thin- and thick-dashed-dotted line), so plasmon modes are damped at a smaller wave vector. Similar behavior has been observed for multilayer graphene structures in previous publications (Hwang & DasSarma, 2009; Vazifehshenas et al., 2010; Badalyan & Peeters, 2012; Khanh & Men, 2018; Men et al., 2019; Men, 2020).
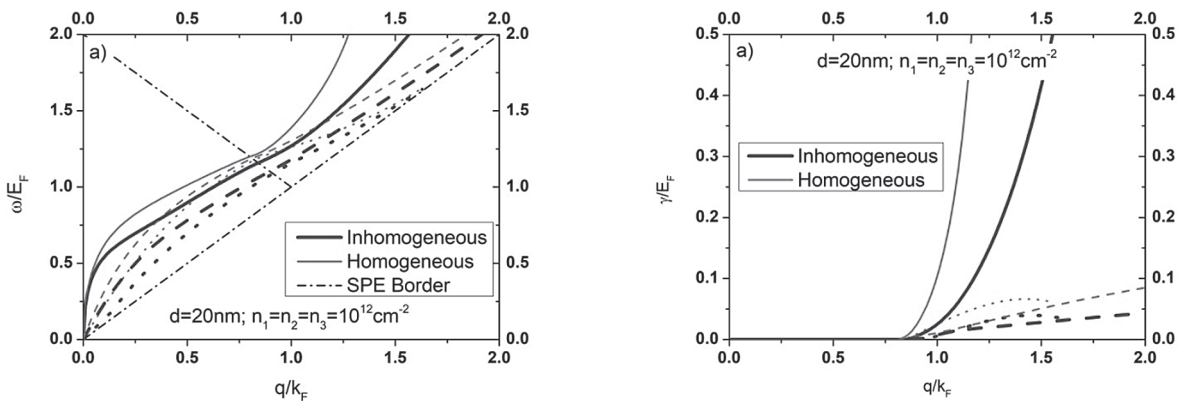
Figure 5. Plasmon modes (a) and damping rate (b) in three-layer graphene structure in homogeneous and inhomogeneous background dielectric, plotted for $d = 20\ nm$ **and** $n_1 = n_2 = n_3 = 10^{12}\ cm^{-2}$. **Dashed-dotted lines present SPE are boundaries**

It is proven that plasmon modes in double layer structures consisting of two graphene sheets grown on an inhomogeneous environment have been studied and published. The results show that plasmon properties in these systems are affected strongly by the inhomogeneity of background dielectric (Badalyan & Peeters, 2012; Khanh & Men, 2018). In order to study the inhomogeneity effects, we plot in Figure 5 plasmon frequencies and the damping rate as a function of the wave vector in the homogeneous and inhomogeneous cases for a comparison. Figure 5(a) demonstrates that plasmon branches in an inhomogeneous system are much lower than those in the homogeneous one (with average permittivity $\bar{\kappa} = (\kappa_1 + \kappa_4)/2 = 2.4$) for the same separation and carrier density. As seen in Figure 5(b) that the inhomogeneity of background dielectric decreases significantly the damping rate of plasma oscillations at a given wave vector in all branches. Finally, plasmon curves in the homogeneous case can merge together at the edge of SPE region with suitable parameters while those in the case of inhomogeneous system are always separated from each other. Similar behaviors have been obtained in previous works for double layer graphene structures (Badalyan & Peeters, 2012; Khanh & Men, 2018).

4. Conclusion

In summary, collective excitations and the damping rate of plasma oscillations in a three-layer graphene structure on inhomogeneous background dielectric within random-phase approximation at zero temperature have been numerical calculated. The results show that three plasmon branches exist in the system including one optical and two acoustic modes. Two higher frequency branches can continue in a single-particle excitation region while the lowest branch merges to the boundary of this region and disappears. The investigations also demonstrate that the increase in interlayer distance reduces significantly the separation between plasmon branches at a given wave vector.

The imbalance in the carrier density in graphene sheets and the inhomogeneity of the environment cause a noticeable decrease in the frequency of plasmon modes.

References

Badalyan, S. M., & Peeters, F. M. (2012). Effect of nonhomogenous dielectric background on the plasmon modes in graphene double-layer structures at finite temperatures. *Physical Review B*, (85), 195444.

DasSarma, S., Adam, S., Hwang, E. H., & Rossi, E. (2011). Electronic transport in two dimensional graphene. *Review Modern Physics,* (83), 407.

Geim, A. K., & Novoselov, K. S. (2007). The rise of graphene. *Nature Mater*, (6), 183.

Hwang, E. H., & DasSarma, S. (2007). Dielectric function, screening, and plasmons in 2D graphene. *Physical Review B*, (75), 205418.

Hwang, E. H., & DasSarma, S. (2009). Exotic plasmon modes of double layer graphene. *Physical Review B*, (80), 205405.

Khanh, N. Q., & Men, N. V. (2018). Plasmon Modes in Bilayer–Monolayer Graphene Heterostructures. *Physica Status Solidi B*, (255), 1700656.

Maier, S. A. (2007). *Plasmonics – Fundamentals and Applications.* New York: Springer.

McCann, E. (2011). *Electronic Properties of Monolayer and Bilayer Graphene*. In: Raza H. (eds) Graphene Nanoelectronics. NanoScience and Technology. Berlin, Heidelberg: Springer. https://doi.org/10.1007/978-3-642-22984-8_8.

Men, N. V., & Khanh, N. Q. (2017). Plasmon modes in graphene–GaAs heterostructures. *Physics Letters A*, (381), 3779.

Men, N. V. (2019). Coulomb bare interaction in

three-layer graphene. Dong Thap University *Journal of Science*, (39), 82-87.

Men, N. V. (2020). Plasmon modes in N-layer gapped graphene. *Physica B, 578*, 411876.

Men, N. V., Khanh, N. Q., & Phuong, D. T. K. (2019). Plasmon modes in N-layer bilayer graphene structures. *Solid State Communications,* (298), 113647.

Phuong, D. T. K., & Men, N. V. (2019). Plasmon modes in 3-layer graphene structures: Inhomogeneity effects. *Physics Letters A*, (383), 125971.

Politano, A., Cupolillo, A., Di Profio, G., Arafat, H. A., Chiarello, G. and Curcio, E. (2016). When plasmonics meets membrane technology. J. *Phys. Condens. Matter*, (28), 363003.

Politano, A., Pietro, A., Di Profio, G., Sanna, V., Cupolillo, A., Chakraborty, S., Arafat, H., & Curcio, E. (2017). Photothermal membrane distillation for seawater desalination. *Advanced Materials*, (29), 03504.

Principi, A., Carrega, M., Asgari, R., Pellegrini, V., & Polini, M. (2012). Plasmons and Coulomb drag in Dirac/Schrodinger hybrid electron systems. *Physical Review B,* (86), 085421.

Ryzhii, V., Ryzhii, M., Mitin, V., Shur, M. S., Satou, A., & Otsuji, T. (2013). Injection terahertz laser using the resonant inter-layer radiative transitions in double-graphene-layer structure. *J. Appl. Phys.*, (113), 174506.

Scharf, B., & Matos-Abiague, A. (2012). Coulomb drag between massless and massive fermions. *Physical Review B,* (86), 115425.

Sensarma, R., Hwang, E. H., & Sarma, S. D. (2010). Dynamic screening and low energy collective modes in bilayer graphene. *Physical Review B,* (82), 195428.

Shin, J-S., Kim, J-S., & Kim, J. T. (2015). Graphene-based hybrid plasmonic modulator. *J. Opt.*, (17), 125801.

Vazifehshenas, T., Amlaki, T., Farmanbar, M., & Parhizgar, F. (2010). Temperature effect on plasmon dispersions in double-layer graphene systems. *Physics Letters A*, (374), 4899.

Yan, H., Li, X., Chandra, B., Tulevski, G., Wu, Y., Freitag, M., Zhu, W., Avouris, P., & Xia, F. (2012). Tunable infrared plasmonic devices using graphene/insulator stacks. *Nature Nanotech.*, (7), 330.

Zhu, J.-J., Badalyan, S. M., & Peeters, F. M. (2013). Plasmonic excitations in Coulomb-coupled N-layer graphene structures. *Physical Review B*, (87), 085401.